CrystEngComm

Accepted Manuscript

ROYAL SOCIETY OF CHEMISTRY

www.rsc.org/crystengcomm

Journal Name

ARTICLE

Unique lanthanide- framework with 6^3 topology based on 1,5-naphthalenedisulfonate and 1H-imidazo[4,5-f][1,10]-phenanthroline: Syntheses, crystal structure, photoluminescence, and white light emission

Received 00th January 20xx,
Accepted 00th January 20xx

DOI: 10.1039/x0xx00000x

www.rsc.org/

Dou Ma,[a] Rui Huo[a] and Xia Li[a*]

Novel lanthanide–organic frameworks $\{[Ln_2(1,5\text{-NDS})_3(IP)_4(H_2O)_2]\cdot 9H_2O\}_n$ (Ln = Pr **1**, Sm **2**, Eu **3**, Gd **4**, Dy **5**, Tb **6**; 1,5-NDS = 1,5-naphthalenedisulfonate, and IP = 1H-imidazo[4,5-f][1,10]-phenanthroline) were synthesized and characterized. The complexes possess unique 2D architectures with 6^3 topology, and their structures consist of three-connected uninodal chain-layer framework with helical characteristics. Complexes **1**, **4**, **5**, and **6** show ligand-based fluorescence, whereas complexes **2** and **3** show typical emission with 4f-4f transitions for Ln(III) ions. Sm(III)-framework (**2**) exhibits a white light emission. The two-component Ln(III) (Gd, Dy, and Pr)-Eu(III)-doped complexes result in white light emission. When Gd(III) ion is incorporated into the Eu(III)-framework with arbitrary ratios of Gd:Eu, white light emission is achieved.

Introduction

The design, synthesis, and characterization of metal–organic frameworks (MOFs) have been intensively studied over the past two decades because of their novel structures and potential applications in chemistry and materials science.[1] lanthanide (Ln)-based MOFs (LnOFs) show a diversity of structure because of their large radii and high coordination number. LnOFs have unique photoluminescence, magnetic and electronic properties, which have been conferred by the $4f^n$ electronic configuration of the Ln(III) ion.[2] Because of their distinct luminescence properties, LnOFs are widely studied for their application in biosensors, immunoassays, and luminescent probes and white light production.[2b–f] The luminescence properties of the different Ln(III) compounds are well-documented.[3] However, by adjusting the doping concentration of Ln(III) ions, luminescent colors can be tuned and white light emission can be achieved. [3–6] The doped Ln(III) complexes are being considered for displays and light-emitting diodes.[4] To date, some white light-emitting LnOFs have been reported, such as the three-component doped LnOFs, La:Eu,Tb, Gd:Eu,Tb, Gd:Dy,Eu, and Sm:Eu,Tb.[5] However, few reports of white light emission by single- and two-component LnOFs were studied.[6] Eu(III) ion is regarded as a promising red-emitting phosphor because of its intense emission at 615 nm via $^5D_0 \rightarrow {}^7F_2$ transition, long emission lifetime, and high emission quantum yield. Therefore, Eu(III) ion is a perfect candidate for designing luminescent MOFs. The application of LnOFs doped with Eu(III) ions to produce white light-emitting materials has attracted much attention.[5,6c–f]

This work aims to construct LnOFs with novel topologies and to investigate white light emission based on the doped Ln(III) complexes. We used 1,5-naphthalenedisulfonate (1,5-NDS) the bridging ligand and incorporated 1H-imidazo[4,5-f][1,10]-phenanthroline (IP) as a co-ligand into the LnOF system. Rigid 1,5-NDS is a bridging multidentate ligand that can bind to Ln(III) ions via different coordination modes.[7] Bidentate IP ligand is incorporated within the backbone of the complexes to improve the luminescence properties.[5d,6c–d] Thus, the new LnOFs (Ln = Pr **1**, Sm **2**, Eu **3**, Gd **4**, Dy **5**, Tb **6**) were obtained. They have unique 2D structures with a Schläfli symbol of 6^3 topology linked left- and right-handed helices. Of these LnOFs, only the Eu(III) and Sm(III) complexes exhibit Ln(III) characteristic emission, and white light emission is achieved by a single-component Sm(III) framework. The other four complexes exhibit ligand fluorescence. The series of doped Eu(III) complexes provided white light emission for the Pr(III), Gd(III), and Dy(III) dopants, respectively. Strikingly, Gd(III)-doped Eu(III)-frameworks with arbitrary concentration ratios of Gd:Eu result in white light emission. To our knowledge, this is the first example of white emitting MOFs.

Experimental section

Materials and general measurements

$Ln(NO_3)_3\cdot 6H_2O$ (Ln = Pr, Sm, Eu, Gd, Dy and Tb) were prepared by the corresponding oxide with nitric acid. Other reagent

[a] *Beijing Key Laboratory for Optical Materials and Photonic Devices, Deparment of Chemistry, Capital Normal University, Beijing 100048. Fax: +86 10 68902320; Tel: +86 10 68902320; E-mail: xiali@.cnu.edu.cn*

† Footnotes relating to the title and/or authors should appear here.
Electronic Supplementary Information (ESI) available: [details of any supplementary information available should be included here]. See DOI: 10.1039/x0xx00000x

were commercially available and were used without further purification.

The elemental analyses (C/H/N) were obtained on a Vario EL elemental analyzer. Infrared (IR) spectra were measured on a Bruker Tensor37 spectrophotometer using the KBr pellets technique. Experimental powder X-ray diffraction (PXRD) was carried out on a PANaytical X' Pert PRO MPD diffractometer with CuK_α radiation (λ = 1.5406 Å), with a scan speed of 2°·min^{-1} and a step size of 0.02° in 2θ. The simulated PXRD patterns were obtained from the single-crystal X-ray diffraction data. Thermogravimetric analyses (TGA) were carried out using a HCT-2 thermal analyzer under air from room temperature to 800 °C with a heating rate of 10 °C/min. Solid state excitation and emission spectra were recorded on an FL4500 fluorescence spectrophotometer (Japan Hitachi company) at room temperature. The fluorescence lifetimes were measured on FLS920 Steady State & Time-resolved Fluorescence Spectrometer (Edinburgh Instrument). The emission quantum yields were measured using a Quantum Yield Measurement System Fluorolog®-3 (HORIBA company) with a 450W Xe lamp coupled to a monochromator for wavelength discrimination, an integrating sphere as sample chamber, and an analyzer R928P for signal detection. The CIE (Commission International de l'Eclairage) color coordinates were calculated on the basis of the international CIE standards.[8]

The X-ray single crystal data collections for the six complexes were performed on a Bruker Smart Apex II CCD diffractometer equipped with a graphite monochromated Mo Kα radiation (λ = 0.71073 Å) at 295(2) K. Semiempirical absorption correction was applied using the SADABS program.[9a] The structures were solved by direct methods and refined by full matrix least squares method on F^2 using SHELXS 97 and SHELXL 97 programs.[9b-c]

Synthesis of complexes 1–6

$\{[Ln_2(1,5\text{-NDS})_3(IP)_4(H_2O)_2]\cdot 9H_2O\}_n$ (Ln = Pr **1**, Sm **2**, Eu **3**, Gd **4**, Dy **5**, Tb **6**). A mixture of $Ln(NO_3)_3\cdot 6H_2O$ (0.1 mmol) (Ln = Pr **1**, Sm **2**, Eu **3**, Gd **4**, Dy **5** and Tb **6**), 1,5-naphthalenedisulfonate (0.15 mmol, 0.0498g), 1H-imidazo[4,5-f][1,10]-phenanthroline(0.1mmol, 0.0220g), 10 mL H_2O and an aqueous solution of NaOH (1 mol/L, 0.10 mL) was sealed into a 25 mL Teflon-lined stainless steel autoclave. The mixture was heated at 180 °C for 3 days. Block-shaped crystals were collected. Yield: 56%-62%. For **1,** Anal. Calc. for $C_{82}H_{62}N_{16}O_{29}S_6Pr_2$: C, 44.57; N, 10.14; H, 2.83%.Found: C, 44.33; N, 9.97; H, 3.16%. Selected IR (KBr pellet, cm^{-1}): 3420(vs) 、 1613(m) 、 1579(m) 、 1542(m) 、 1425(m) 、 1395(s)、1268(s)、1226(s)、1198(s)、1168(s)、1144(vs)、1082(m)、1033(vs)、1021(vs)、792(s)、767(m)、734(m)、611(vs)、567(m)、522(w)、467(w)、415(w). For **2**, Anal. Calc. for $C_{82}H_{62}N_{16}O_{29}S_6Sm_2$: C, 44.19; N, 10.06; H, 2.80%.Found: C, 43.85; N, 9.88; H, 3.22%. Selected IR (KBr pellet, cm^{-1}): 3413(vs) 、 1613(m) 、 1560(m) 、 1542(m) 、 1426(m) 、 1394(s)、1269(s)、1227(s)、1198(s)、1167(s)、1145(vs)、1083(m)、1030(vs)、1021(vs)、792(s)、767(m)、733(m)、611(vs)、568(m)、522(w)、466(w)、415(w). For **3**, Anal. Calc. for $C_{82}H_{62}N_{16}O_{29}S_6Eu_2$: C, 44.04; N, 10.04; H, 2.80%.Found: C, 43.77; N, 9.87; H, 3.12%. Selected IR (KBr pellet, cm^{-1}): 3433(vs) 、 1613(m) 、 1579(m) 、 1542(m) 、 1425(m) 、 1398(s)、1269(s)、1226(s)、1198(s)、1167(s)、1145(vs)、1083(m)、1035(vs)、1021(vs)、949(w)、792(s)、767(m)、736(m) 、 691(w) 、 662(w) 、 611(vs) 、 567(m) 、 522(w) 、 416(w). For **4,** Anal. Calc. For $C_{82}H_{62}N_{16}O_{29}S_6Gd_2$: C, 43.92; N, 9.99; H, 2.79%.Found: C, 43.44; N, 9.77; H, 3.26%. Selected IR (KBr pellet, cm^{-1}): 3429(vs)、1611(m)、1579(m)、1542(m)、1425(m)、1397(s)、1270(s)、1227(s)、1198(s)、1167(s)、1145(vs)、1083(m)、1027(vs)、1021(vs)、792(s)、766(m)、738(m)、611(vs)、568(m)、521(w)、415(w). For **5,** Anal. Calc for $C_{82}H_{62}N_{16}O_{29}S_6Dy_2$: C, 43.72; N, 9.95; H, 2.77%.Found: C, 43.29; N, 9.79; H, 3.30%. Selected IR (KBr pellet, cm^{-1}): 3431(vs) 、 1614(m) 、 1581(m) 、 1543(m) 、 1425(m) 、 1396(s)、1270(s)、1227(s)、1198(s)、1166(s)、1145(vs)、1084(m)、1028(vs)、1021(vs)、792(s)、767(m)、733(m)、611(vs)、573(m)、521(w)、416(w). For **6,** Anal. Calc. for $C_{82}H_{62}N_{16}O_{29}S_6Tb_2$: C, 43.66; N, 9.98; H, 2.78%.Found: C, 43.11; N, 9.78; H, 3.18%. Selected IR (KBr pellet, cm^{-1}): 3426(vs) 、 1611(m) 、 1576(m) 、 1543(m) 、 1425(m) 、 1397(s)、1269(s)、1225(s)、1198(s)、1170(s)、1143(vs)、1082(m)、1028(vs)、1021(vs)、792(s)、767(m)、735(m)、610(vs)、567(m)、520(w)、415(w).

For Pr/Gd/Dy,Eu-doped coordination network, the synthetic method is same as mentioned above just by loading the corresponding $Ln(NO_3)_3\cdot 6H_2O$ as the starting materials in stoichiometric ratios. The doped materials are isostructural to the original complexes (**1**-**6**) verified by powder X-ray diffraction (PXRD) analysis, their PXRD patterns match the those of **1**-**6** (Fig. S1).

Results and discussion

Crystal Structures

The complexes $\{[Ln_2(1,5\text{-NDS})_3(IP)_4(H_2O)_2]\cdot 9H_2O\}_n$ (Ln = Pr **1**, Sm **2**, Eu **3**, Gd **4**, Dy **5**, Tb **6**) are isostructural (Table 1, Fig. S1) and show layer framework. Comparing the average distances (Table S1) of the Ln–O, Ln–N, and Ln···Ln for the complexes **1**-**6**, the corresponding distances decrease with decreasing ionic radius of the Ln(III) ions (Pr(III) > Sm(III) > Eu(III) > Gd(III) > Tb(III) > Dy(III)). This order is consistent with lanthanide contraction. Complex **3** is selected as an example to describe the structure. The asymmetric unit of **3** comprises one Eu(III) ion, one and one-half 1,5-NDS ligands, two IP ligands, one water molecule, and free water molecules. Each Eu(III) ion is bound to four nitrogen atoms (N1, N2, N5, and N6) from the two IP ligands, one water molecule (O10), and three oxygen atoms (O1, O4, and O7) from the three 1,5-NDS ligands in a distorted $[EuO_4N_4]$ square antiprism arrangement (Fig. 1a). The Eu-O (sulfonate) distances range from 2.317(5) to 2.347(5) Å, and the Eu-N distances range from 2.587(6) to 2.622(6) Å. The Eu-O (water) bond length is 2.356(5) Å. Each sulfonate group uses one of its three oxygen atoms to coordinate with the Eu(III) ion. The two coordinated terminal IP ligands are nearly

Table **1** Crystallographic and refinement data for complexes **1**-**6**.

Complex	**1**	**2**	**3**	**4**	**5**	**6**
Empirical formula	$C_{82}H_{62}N_{16}O_{29}S_6Pr_2$	$C_{82}H_{62}N_{16}O_{29}S_6Sm_2$	$C_{82}H_{62}N_{16}O_{29}S_6Eu_2$	$C_{82}H_{62}N_{16}O_{29}S_6Gd_2$	$C_{82}H_{62}N_{16}O_{29}S_6Dy_2$	$C_{82}H_{62}N_{16}O_{29}S_{6}$
Formula weight	2209.66	2228.54	2231.76	2242.34	2252.84	2245.68
Crystal system	Monoclinic	Monoclinic	Monoclinic	Monoclinic	Monoclinic	Monoclinic
space group	*P2(1)/c*	*P2(1)/c*	*P2(1)/c*	*P2(1)/c*	*P2(1)/c*	*P2(1)/c*
a(Å)	17.3644(8)	17.3435(16)	17.3174(17)	17.2968(15)	17.2852(19)	17.2839(8)
b(Å)	16.2122(8)	16.1923(16)	16.1834(16)	16.1959(14)	16.1853(17)	16.1782(6)
c(Å)	16.2003(8)	16.0934(14)	16.0660(14)	16.0280(14)	15.9746(17)	16.0035(6)
β(°)	103.5170(10)	103.429(2)	103.431(2)	103.363(2)	103.335(2)	103.3160(
Volume ($Å^3$)	4434.3(4)	4396.0(7)	4379.4(7)	4368.5(7)	4348.7(8)	4354.6(3)
Z	2	2	2	2	2	2
Calculated density / g· cm^{-3}	1.655	1.684	1.692	1.705	1.720	1.713
Absorption coefficient/ mm^{-1}	1.318	1.557	1.655	1.741	1.942	1.848
F(000)	2224	2236	2240	2244	2252	2248
Crystal size / mm^3	0.40x0.20x0.15	0.35x0.18x0.13	0.38x0.22x0.10	0.35x0.15x0.10	0.40x0.15x0.10	0.38x0.16x0.1
θ range for data collection / (°)	1.74 to 25.25	1.74 to 25.25	1.75 to 25.25	1.75 to 25.25	1.75 to 25.25	1.75 to 25.25
Limiting indices	-20≦h≦10; -19≦k≦19; -19≦l≦19	-20≦h≦20; -15≦k≦19; -15≦l≦19	-20≦h≦20; -19≦k≦19; -19≦l≦19	-10≦h≦20; -19≦k≦19; -19≦l≦18	-20≦h≦20; -19≦k≦12; -17≦l≦19	-17≦h≦20; -16≦k≦19; -16≦l≦19
Reflections collected/unique	[R(int)= 0.0395] 21418 / 8002	[R(int)= 0.0767] 19461 / 7797	[R(int)= 0.1043] 21852 / 7928	[R(int)= 0.0578] 19044/ 7796	[R(int)= 0.0457] 20472/ 7874	[R(int)= 0.051 24267 / 788
Data / restraints / parameters	8002 / 3 / 620	7797 / 3 / 620	7928 / 3 / 620	7796 / 3 / 620	7874 / 3 / 620	7889 / 3 / 62
Goodness-of-fit on F^2	1.228	1.021	1.006	1.028	1.089	1.063
Final R indices[I>2sigma(I)]	R1 = 0.0393 wR2 =0.0865	R1 = 0.0552 wR2 =0.0968	R1 = 0.0571 wR2 =0.1033	R1 = 0.0475 wR2 =0.0875	R1 = 0.0387 wR2 =0.0814	R1 = 0.0375 wR2 =0.076
R indices(all data)	R1 = 0.0551 wR2 = 0.0930	R1 = 0.1014 wR2 = 0.1134	R1 = 0.1126 wR2 =0.1233	R1 = 0.0797 wR2 =0.0996	R1 = 0.0574 wR2 =0.0889	R1 = 0.0600 wR2 =0.08
Largest difference peak and hole / e.$Å^{-3}$	1.054 and -0.432	0.863 and -0.593	0.695 and -0.726	0.822 and -0.681	0.918 and -0.516	0.844 and -0.4
CCDC No.	1060203	1060204	1060205	1060206	1060207	1060208

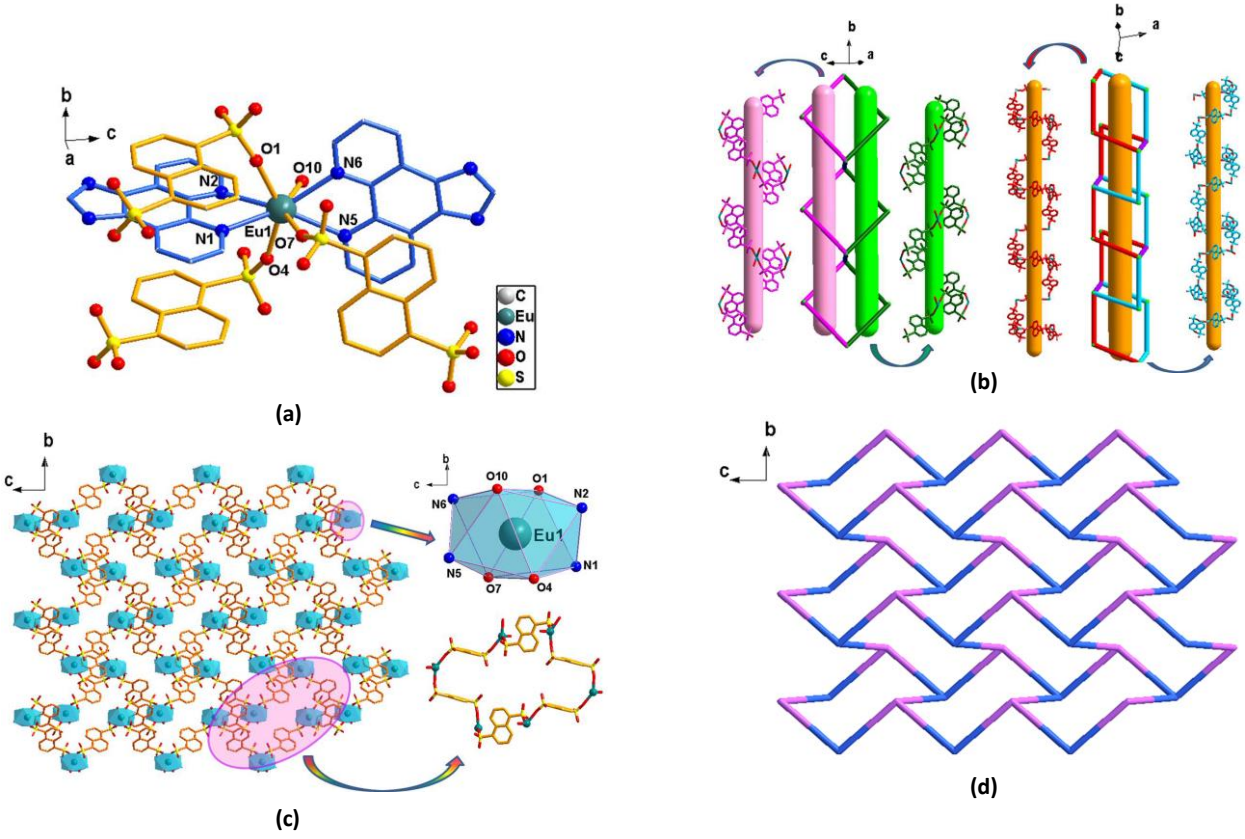

Fig. 1 View of the structure of **3**: (a) Coordination environment of Eu(III), (b) The helix chains, (c) 2D structure, (d) $\{6^3\}$ topology net.

orthogonal, with a dihedral angle of 82.089(6)° to minimize steric interactions. The terminal IP ligands seem to prevent the formation of a 3D framework. The 1,5-NDS ligand acts as linear linker between two Eu(III) ions. Each Eu(III) ion is connected by three 1,5-NDS ligands, resulting in three Eu-(1,5-NDS) zigzag chains with a Eu···Eu separation of 10.889 Å along three different directions. It is noteworthy that there are two types of Eu-(1,5-NDS)n helices. One helix has a repeat unit consisting of four Eu(III) centers and four 1,5-NDS ligands with a pitch of 39.862 Å. Other helix has a repeat unit consisting of six Eu(III) centers and six 1,5-NDS ligands with a pitch of 22.804 Å (Fig. 1b). Both left-handed and right-handed helices are interconnected by sharing the $[EuO_4N_4]$ polyhedra to form a layer structure, in which the six Eu(III) ions and six 1,5-NDS ligands form a hexagonal grid-like structure (Fig. 1c). In the structure, Eu(III) ions are not on the same plane. The $[EuO_4N_4]$ unit can be classified as a three-connected node. The most fascinating structural feature of **3** is that analysis with TOPOS software[10] reveals a 3-connected uninodal net with a $\{6^3\}$ topology (Fig. 1d), which is different from the $\{6^3\}$ topology net reported in literatures.[11] The packing diagram reveals that the 2D layers are connected by intermolecular weak interactions, thereby forming a 3D supermolecule structure (Fig. S2). Hydrogen bonds O-H···N are present from coordinated water to IP with an O10-N7 separation of 2.7376(8) Å and an angle of 171.734(4)°. The free water molecules are present in the cavity of 3D supermolecule structure.

The thermogravimetric analysis curve of **3** exhibits two main stages of weight loss (Fig. S3). The first stage occurs in the temperature range of 41-276 °C, corresponding to the release of water molecules. The observed weight loss of 8.83% is close to the calculated value of 8.88%. The second stage starts at 394 °C and is completed at 582 °C, thereby, final residual is Eu_2O_3. The total observed weight loss of 79.40% is close to the calculated value of 84.23%, which corresponds to the decomposition of organic ligands.

Luminescent Properties

The fluorescent spectra of the complexes and the free ligands in the solid state were obtained at room temperature. The emission spectra of the ligands present broad bands that are centered at 392 nm for 1,5-NDS and at 468 nm, with shoulder peaks at 453 nm and 523 nm, for IP (Fig. 2a and 2b). The broad bands are attributed to the typical π*-π transitions. Under excitation at 365 nm, complexes **1**, **4**-**6** exhibit broad and strong blue-green emissions that are centered at 423, 461, and 481 nm for **1**, 472 nm for **4**, 500 nm for **5,** and 491 nm for **6** (Fig. 2c,d,e,f). The broad bands coincide with a ligand-based emission, indicating that the fluorescence of complexes **1**, **4**-**6** comes from the ligands. The emission spectra of **1**, **4**-**6** do not show the characteristic emissions for Pr(III), Gd(III), Dy(III), and Tb(III) ions probably because of the mismatch of the energy levels between the triplet state of the ligands and the excited state of the Ln(III) ions. The Gd(III) ion is typically known to be located at 32150 cm^{-1} . Its characteristic f-f transitions are not

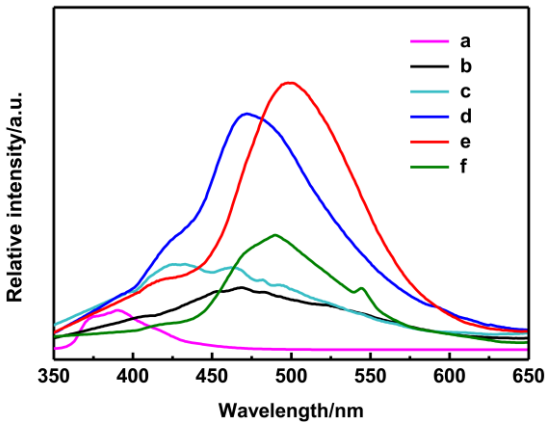

Fig. 2 Emission spectra of 1,5-NDS(a), IP(b), **1**(c), **4**(d), **5**(e) and **6**(f).

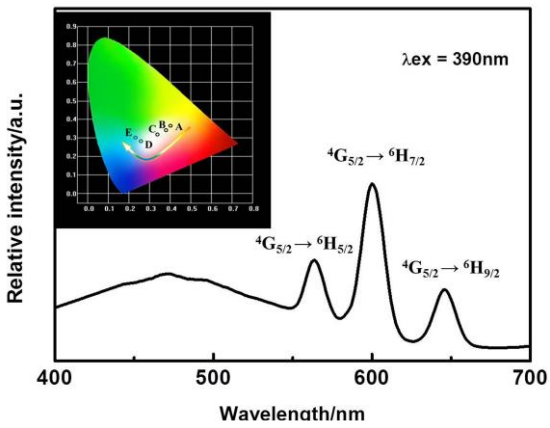

Fig. 3 Emission spectrum of **2**. Inset: the CIE chromaticity diagram. A(λex = 340nm), B(λex = 380nm), C(λex = 390nm), D(λex = 400nm), E(λex = 410nm).

visible. The emissions of **1**, **4**-**6** are more intense than that of the free ligands, and such intensity may be explained by differences in rigidity.[5c,12] Compared with the luminescence feature of the ligands in **1** and **4**-**6**, it reveals that the ligand emission is dependent on the nature of Ln(III) ions. A different-shift for **1** and **4**-**6**, with respect to the ligand emission bands, is observed, which reveals that the ligand possess an interesting environment dependent luminescence emission. The CIE coordinates are (0.218, 0.231) for **1**, (0.211, 0.288) for **4**, (0.211, 0.374) for **5** and (0.208, 0.340) for **6** (Fig. S4).

The emission spectrum of **2** exhibits narrow bands at 563 nm (green), 598 nm (orange), and 642 nm (red) (Fig. 3), corresponding to the $^4G_{5/2}\rightarrow {}^6H_{5/2}$, $^4G_{5/2}\rightarrow {}^6H_{7/2}$, and $^4G_{5/2}\rightarrow {}^6H_{9/2}$ transitions of Sm(III), respectively, upon excitation of UV wavelengths of 300–420 nm. Furthermore, a broad band that centers at 464 nm in the blue region (420-520 nm) is present because of the emission from the ligands. The tunable emission is obtained by varying the excitation wavelengths and is characterized by chromaticity coordinates in a Commission on Illumination (CIE) chromaticity diagram (Fig. 3, inset). The chromaticity coordinates gradually move from yellow region to blue region with increasing excitation wavelength. White light emission is obtained at excitation wavelengths of 340-390 nm. When excited at 390 nm, the CIE (0.328, 0.321) is very close to the standard white light (0.333, 0.333), according to the 1931 CIE coordinate diagram. The color rendering index (CRI) and correlated color temperature (CCT) are 84 and 5722 K, respectively. The lifetime of Sm(III) emission is 19.8 μs for **2** (Fig. S5)**.** Thus, both remaining ligand fluorescence and the Sm(III)-centered luminescence are incorporated into the white light emission. The result indicates that Sm(III)-complex can be used as a single-component white light-emitting material. White light emission from a single-component phosphor is expected for high quality white light sources. However, single-phase white light emitting MOFs has seldom been achieved.[6a–c] In the excitation spectrum (Fig. 4, inset) of **3**, which is monitored at an emission wavelength of 613 nm, the strong broad band centered at 376 nm can be attributed to the excited levels of the ligand, proving that the luminescence sensitization via excitation of the ligand is effective. Under excitation at 376 nm, the emission spectrum of **3** exhibits sharp bands at 591, 613, 650 and 696 nm, which are attributed to the transitions of $^5D_0\rightarrow {}^7F_J$ with J = 1, 2, 3, and 4, respectively (Fig. 4). Two main characteristic peaks from $^5D_0\rightarrow {}^7F_2$ (red, 613nm) and $^5D_0\rightarrow {}^7F_1$ (orange, 591 nm) are dominant. The intensity ratio of 1.96 for $I(^5D_0\rightarrow {}^7F_2):I(^5D_0\rightarrow {}^7F_1)$ indicates that the coordinating environment of the Eu(III) ion in **3** lacks an inversion center.[13] In addition, a very weak ligand broad emission band centered at 467 nm is observed in **3**, indicating sizable energy transfer from ligands to the $^5D_0$ level of Eu(III).[14] The $^5D_0$ (Eu(III)) decay curve is monitored within the $^5D_0\rightarrow {}^7F_2$ transition (Fig. S6). The observed luminescence decay profile corresponds to a single exponential function, implying the presence of only one emissive Eu(III) center. The lifetime of Eu(III) emission is 0.320 ms for **3.**

The tricolor combination (red, green, and blue) can show white light emission. Developing white light potential in general lighting applications, is desirable. White light emission can be obtained by doping Gd(III), Pr(III), and Dy(III) ions into the Eu(III) complex, respectively, because Gd(III), Pr(III), and Dy(III) complexes display blue-green light emission, which is

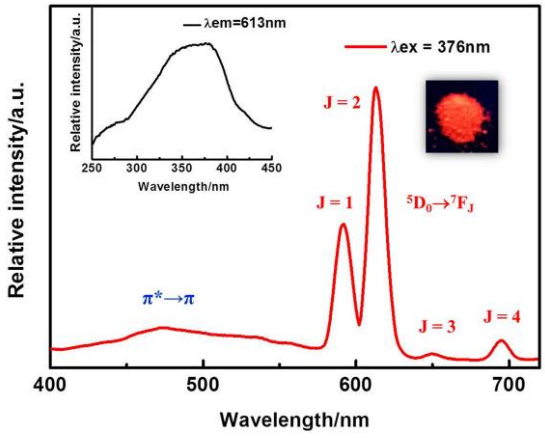

Fig. 4 Emission spectrum of **3.** Inset: excitation spectrum, image of **3** by 365nm light.

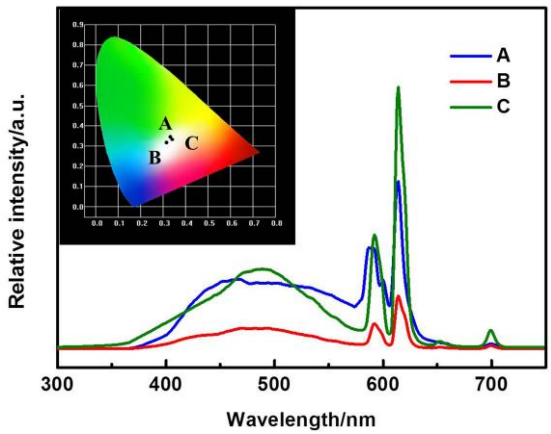

Fig. 5 Emission spectra of $Gd_{0.90}Eu_{0.10}$ (A,λex = 350nm), $Pr_{0.80}Eu_{0.20}$ (B, λex = 340nm) and $Dy_{0.80}Eu_{0.20}$ (C, λex = 390nm) doped complexes. Inset: the CIE chromaticity diagram.

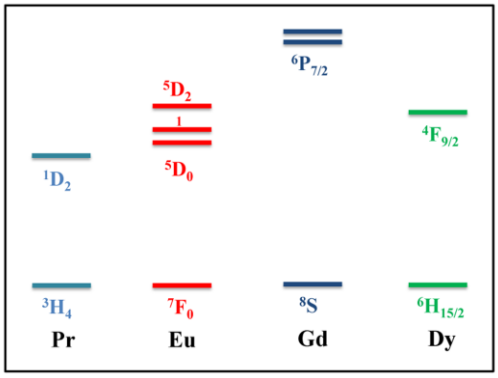

Scheme. 1 A diagram of some chosen energy levels for Ln(III) ions (Ln = Pr, Eu, Gd, Dy).

the complementary color of red emission from the Eu(III) ion. The ionic radii of Ln(III) ions (Pr(III), 101 pm; Gd(III), 94 pm; and Dy(III), 91 pm) are comparable to that of Eu(III) (98 pm).These Ln(III) ions also have similar coordination geometries. Thus, Pr(III), Gd(III), and Dy(III) were doped separately into Eu(III) complex, and generating the $Gd_{0.90}Eu_{0.10}$, $Pr_{0.80}Eu_{0.20}$, and $Dy_{0.80}Eu_{0.20}$ doped complexes are attempted (Fig. S1). The emission spectra (Fig. 5) of $Gd_{0.90}Eu_{0.10}$, $Pr_{0.80}Eu_{0.20}$, and $Dy_{0.80}Eu_{0.20}$ doped materials are similar, except for their intensities under UV light. The sharp main emission peaks at 592 and 613 nm, are attributed to transitions of $^5D_0 \rightarrow {}^7F_J$ (J = 1, 2) of Eu(III) ion and broad emission band in the region of 420-550 nm is from the ligands. When $Gd_{0.90}Eu_{0.10}$, $Pr_{0.80}Eu_{0.20}$, and $Dy_{0.80}Eu_{0.20}$ are excited at 350, 340, and 390 nm, respectively, the CIE coordinates A (0.330, 0.332) (CRI 87, CCT 5587 K), B (0.310, 0.300) (CRI 66, CCT 6983 K), and C (0.335, 0.310) (CRI 63, CCT 5344 K) for $Gd_{0.90}Eu_{0.10}$, $Pr_{0.80}Eu_{0.20}$, and $Dy_{0.80}Eu_{0.20}$ doped complexes, respectively, are very close to the CIE coordinates of the standard white light (0.333, 0.333), according to the CIE 1931 coordinate diagram. Consequently, white light emission is achieved by Gd-Eu, Pr-Eu, and Dy-Eu doped complexes under the broad UV region. Obviously, the selected excitation wavelengths for white light emission decrease in order of the Dy-Eu, Gd-Eu, Pr-Eu doped complexes. The Gd-Eu doped complex exhibits better chromaticity coordinates, higher CRI, corresponding with high-quality white light illumination requirements.[6c,f]

Spectral comparison in Fig. 5 shows that co-doping with a small amount of Dy(III) ion enhances the Eu(III) emission while co-doping with a small amount of Pr(III) ion decreases the Eu(III) emission. An energy level has been given in scheme. 1 for explaining the emission mechanisms of the complexes. The energy level ($^4F_{9/2}$) of Dy(III) (21.14 X 10^3 cm^{-1}) is higher than the energy level $^5D_0$ of Eu(III) (17.29 X 10^3 cm^{-1}), the energy transfer (ET) is possible due to the nonradiative relaxation from $^4F_{9/2}$ level of Dy(III) to the $^5D_0$ level of Eu(III).[2a] Thereby co-doping with a small amount of Dy(III) ion enhances the Eu(III) emission in the Dy-Eu doped complex. However, the energy level $^1D_2$ of Pr(III) (17.00 X 10^3 cm^{-1}) is lower than the energy level $^5D_0$ of Eu(III) (17.29 X 10^3 cm^{-1}), the ET is possible due to the nonradiative relaxation from $^5D_0$ level of Eu(III) to the $^1D_2$ level of Pr(III).[2a] Furthermore, the Pr(III) ion has many excited levels resulting in an energy transfer from the ligands to the energy levels of the Pr(III) ion. These weaken energy transfer from the ligands to Eu(III) ion, thus leading to the decrease of Eu(III) emission in the Pr-Eu doped complex. The lifetimes (τ) for the most intense emission lines (613 nm of Eu(III) ($^5D_0 \rightarrow {}^7F_2$) in the doped complexes are also recorded (Fig. S7, Table S2). These decay curves correspond to a single exponential behavior, which indicates the homogeneous distribution of doping ions inside the doped complexes.[15] The lifetime values of $^5D_0$ Eu(III) are 0.348, 0.339 and 0.202 ms in the Dy-Eu, Gd-Eu and Pr-Eu doped complexes, respectively. The quantum yields (QY) of white light emission are 2.25%, 2.22% and 1.18% for the Dy-Eu, Gd-Eu, Pr-Eu doped complexes. The lifetime values and the quantum yields of white light emission are gradually increased in order of Dy-Eu, Gd-Eu and Pr-Eu doped complexes. These results are in agreement with emission discussed above.

The quality of the white light for $Gd_{0.90}Eu_{0.10}$ doped complex is superior to that for $Pr_{0.80}Eu_{0.20}$ and $Dy_{0.80}Eu_{0.20}$ doped complexes, implying that the Gd(III) complex is a better matrix

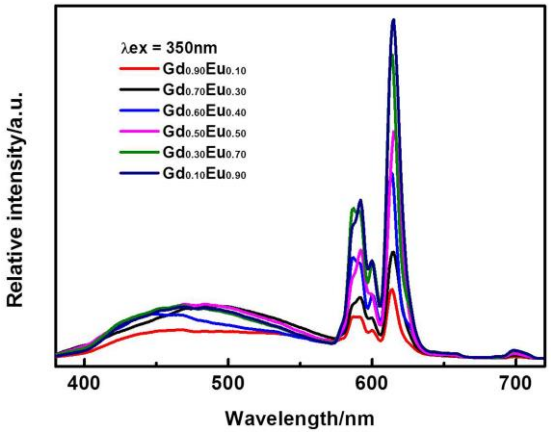

Fig. 6 Emission spectra of $Gd_{1.0-x}Eu_x$ (x= 0.1, 0.3, 0.4, 0.5, 0.7, 0.9) doped complexes.

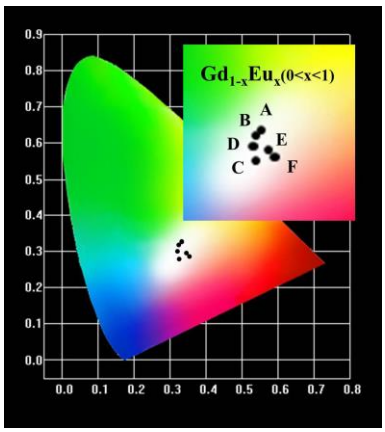

Fig. 7 The CIE chromaticity diagram of $Gd_{1.0-x}Eu_x$ doped complexes. A(x = 0.1, λex = 350 nm), B(x = 0.3, λex = 360nm), C(x = 0.4, λex = 300 nm), D(x = 0.5, λex = 300 nm), E(x = 0.7, λex = 300 nm), F(x = 0.9, λex = 280 nm).

Table **2** The CIE data of $Gd_{1.0-x}Eu_x$ doped complexes

	Complex	λex/nm	CIE(x,y)	CCT/K	CRI
A	$Gd_{0.90}Eu_{0.10}$	350	(0.330, 0.332)	5586	87
B	$Gd_{0.70}Eu_{0.30}$	360	(0.325, 0.321)	6004	80
C	$Gd_{0.60}Eu_{0.40}$	300	(0.325, 0.285)	5984	69
D	$Gd_{0.50}Eu_{0.50}$	300	(0.325, 0.301)	5920	69
E	$Gd_{0.30}Eu_{0.70}$	300	(0.345, 0.300)	4852	66
F	$Gd_{0.10}Eu_{0.90}$	280	(0.355, 0.296)	4256	61

for obtaining white light- emitting material. To further investigate the emission properties of Gd-Eu doped complexes, a series of $Gd_{1.0-x}Eu_x$ (x = 0.1, 0.3, 0.4, 0.5, 0.7, 0.9) samples were synthesized, and their luminescent spectra were collected under varying UV light excitations from 330 nm to 410 nm. These samples show emissions at 592 and 613 nm of Eu(III) ion and a broad emission band in the 400-550 nm region of the ligands (Fig. 6). These samples present different emission intensities depending on the ratios of the Gd(III) and Eu(III) ions. The emission intensity of the Eu(III) increases with increasing Eu(III) concentration. Strikingly, the emission colors of all samples are located at the white light region (Table 2 and Fig. 7), indicating that the Gd-Eu doped complexes with arbitrary ratios may achieve white light emission. The $Gd_{1.0-x}Eu_x$ (0<x<1) doped complex is the first example of white light emitting MOFs that can be produced without considering the doping ratio, thereby simplifying the preparation of white light-emitting MOFs.

Conclusions

A series of LnOFs with arenedisulfonates and IP as a co-ligand were synthesized and characterized. The LnOFs adopt a unique 6^3 topology net with helical characteristics. White light emission was realized by single component Sm(III) framework and two - component Ln(III) doped Eu(III) frameworks (Gd-Eu, Dy-Eu, and Pr-Eu), respectively. Furthermore, white light emission is achieved by using a wide range of excitation wavelengths. Notably, Gd(III) doped Eu(III)-white light emitting material without considering the doping ratio is successfully prepared, which provides easy solution to achieve easily manipulated, low-cost and higher quality white-light.

Acknowledgements

The authors are grateful to the National Natural Science Foundation of China (21471104), the Science and Technology Program, Beijing Municipal Education Commission (KM201510028006) and Scientific Research Base Developme... Program of the Beijing Municipal Commission of Educatio... Thanks the Dr. Hong-Liang Han from Capital Normal University for helpful work and discussions.

Notes and references

1 (a) H. C. Zhou, J. R. Long and O. M. Yaghi, *Chem. Rev.*, 201... **112**, 673; (b) E. Coronado and G. M. Espallargas, *Chem. Soc. Rev.*, 2013, **42**, 1525; (c) J. R. Li, J. Sculley and H. C. Zhou, *Chem. Rev.*, 2012, **112**, 869; (d) L. E. Kreno, K. Leong, O. K. Farha, M. Allendorf, R. P. Van Duyne and J. T. Hupp, *Chem. Rev.*, 2012, **112**, 1105; (e) J. Lee, O. K. Farha, J. Roberts, K. A. Scheidt, S. T. Nguyen and J. T. Hupp, *Chem. Soc. Rev.*, 2009, **38**, 1450.

2 (a) M. D. Allendorf, C. A. Bauer, R. K. Bhakta and R. J. T. Houk *Chem. Soc. Rev.*, 2009, **38**, 1330; (b) Y. J. Cui, B. L. Chen and G. D. Qian, *Coord. Chem. Rev.*, 2014, **273**, 76; (c) J. C. G. Bunzli and C. Piguet, *Chem. Soc. Rev.*, 2005, **34**, 1048; (d) Z. Zhang, Y. Song, T. Okamura, Y. Hasegawa, W. Y. Sun and N. Ueyama, *Inorg. Chem.*, 2006, **45**, 2896; (e) B. D. Chandler, D. T. Cramb and G. K. H. Shimizu, *J. Am. Chem. Soc.*, 2006, **128**, 10403; (f) S. Petoud, S. M. Cohen, J. C. G. Bunzli and K. N. Raymond, *J. Am. Chem. Soc.*, 2003, **125**, 13324.

3 (a) A. Balamurugan, M. L. P. Reddy and M. Jayakannan, *J. Phys. Chem. B*, 2009, **113**, 14128; (b) M. M. Shang, D. L. Geng, X. J. Kang, D. M. Yang, Y. Zhang and J. Lin, *Inorg. Chem.*, 2012, **51**, 11106; (c) D. L. Geng, M. M. Shang, D. M. Yang, Y. Zhang, Z. Y. Cheng and J. Lin, *J. Mater. Chem.*, 2012, **22**, 23789; (d) B. H. Kwon, H. S. Jang, H. S. Yoo, S. W. Kim, D. S. Kang, S. Maeng, D. S. Jang, H. Kim and D. Y. Jeon, *J. Mater. Chem.*, 2011, **21**, 12812; (e) C. H. Huang and T. M. Chen, *Inorg. Chem.*, 201..., **50**, 5725.

4 P. Falcaro and S. Furukawa, *Angew. Chem., Int. Ed.*, 2012, **51**, 8431.

5 (a) S. Dang, J. H. Zhang and Z. M. Sun, *J. Mater. Chem.*, 2012, **22**, 8868; (b) A. R. Ramya, S. Varughese and M. L. P. Reddy, *Dalton Trans.*, 2014, **43**, 10940; (c) D. Ma, X. Li and R. Huo, *J. Mater. Chem. C*, 2014, **2**, 9073; (d) S. Song, X. Li, Y. H. Zhan..., R. Huo and D. Ma, *Dalton Trans.*, 2014, **43**, 5974; (e) X. T. R... Q. Huang, X. L. Yang, Y. J. Cui, Y. Yang, C. D. Wu, B. L. Chen and G. D. Qian, *J. Mater. Chem.*, 2012, **22**, 3210; (f) H. B. Zhang, X. C. Shan, L. J. Zhou, P. Lin, R. F. Li, E. Ma, X. G. Guo and S. W. Du, *J. Mater. Chem. C*, 2013, **1**, 888.

6 (a) Q. Y. Yang, K. Wu, J. J. Jiang, C. W. Hsu, M. Pan, J. M. Lehn and C. Y. Su, *Chem. Commun.*, 2014, **50**, 7702; (b) G. J. He, D. Guo, C. He, X. L. Zhang, X. W. Zhao and C. Y. Duan, *Angew. Chem., Int. Ed.*, 2009, **48**, 6132; (c) Y. H. Zhang, X. Li and S.

Song, *Chem. Commun.*, 2013, **49**, 10397; (d) S. Song, X. Li and Y. H. Zhang, *Dalton Trans.*, 2013, **42**, 10409; (e) Y. Q. Wei, Q. H. Li, R. J. Sa and K. C. Wu, *Chem. Commun.*, 2014, **50**, 1820; (f) F. M. Zhang, P. F. Yan, H. F. Li, X. Y. Zou, G. F. Hou and G. M. Li, *Dalton Trans.*, 2014, **43**, 12574.

7 (a) N. Snejko, C. Cascales, B. Gomez-Lor, E. Gutierrez-Puebla, M. Iglesias, C. Ruiz-Valero and M. A. Monge, *Chem. Commun.*, 2002, 1366; (b) J. P. Zhao, B. W. Hu, F. C. Liu, X. Hu, Y. F. Zeng and X. H. Bu, *CrystEngComm*, 2007, **9**, 902; (c) J. L. Nicholls, S. E. Hulse, S. K. Callear, G. J. Tizzard, R. A. Stephenson, M. B. Hursthouse, W. Clegg, R. W. Harrington and A. M. Fogg, *Inorg. Chem.*, 2010, **49**, 8545; (d) F. Gandara, A. Garcia-Cortes, C. Cascales, B. Gomez-Lor, E. Gutierrez-Puebla, M. Iglesias, A. Monge and N. Snejko, *Inorg. Chem.*, 2007, **46**, 3475; (e) F. Gandara, C. Fortes-Revilla, N. Snejko, E. Gutierrez-Puebla, M. Iglesias and M. A. Monge, *Inorg. Chem.*, 2006, **45**, 9680; (f) K. Banerjee, S. Roy and K. Biradha, *Cryst. Growth Des.*, 2014, **14**, 5164.

8 T. Smith; J. Guild, *Trans Opt. Soc.,* 1931, **33**, 73.

9 (a) G. M. Sheldrick, SADABS, Program for Empirical Absorption Correction of Area Detector Data, University of Götingen, Götingen, Germany, 1997; (b) G. M. Sheldrick, SHELXS-97, Program for Crystal Structure Refinement, University of Göttingen (1997); (c) G. M. Sheldrick, SHELXL-97, Program for Crystal Structure Solution, University of Göttingen (1997).

10 V. A. Blatov, L. Carlucci, G. Ciani and D. M. Proserpio, *CrystEngComm*, 2004, **6**, 377.

11 (a) X. H. Yan, Z. H. Cai, C. L. Yi, W. S. Liu, M. Y. Tan and Y. Tang, *Inorg. Chem.*, 2011, **50**, 2346; (b) Y. L. Lu, J. Y. Wu, M. C. Chan, S. M. Huang, C. S. Lin, T. W. Chiu, Y. H. Liu, Y. S. Wen, C. H. Ueng, T. M. Chin, C. H. Hung and K. L. Lu, *Inorg. Chem.*, 2006, **45**, 2430; (c) J. Q. Sha, L. Huang, J. Peng, H. J. Pang, A. X. Tian, P. P. Zhang, Y. A. Chen and M. Zhu, *Solid. State. Sci.*, 2009, **11**, 417; (d) F. Y. Cui, X. Y. Ma, C. Li, T. Dong, Y. Z. Gao, Z. G. Han, Y. N. Chi and C. W. Hu, *J. Solid. State. Chem.*, 2010, **183**, 2925; (e) X. P. Ye, W. J. Liu, N. Wang and S. T. Yue, *J. Coord. Chem.*, 2013, **66**, 191.

12 J. Z. Gu, Z. Q. Gao and Y. Tang, *Cryst. Growth Des.*, 2012, **12**, 3312.

13 X. F. Huang, J. X. Ma and W. S. Liu, *Inorg. Chem.*, 2014, **53**, 5922.

14 L. Yan, Q. Yue, Q. X. Jia, G. Lemercier and E. Q. Gao, *Cryst. Growth Des.*, 2009, **9**, 2984.

15 Subrata Das, A. Amarnath Reddy, G. Vijaya Prakash, *Ceramics International,* 2012, **38**, 5769.

Unique lanthanide- framework with 6^3 topology based on 1,5-naphthalenedisulfonate and 1H-imidazo[4,5-f][1,10]-phenanthroline: Syntheses, crystal structure, photoluminescence, and white light emission

Dou Ma, Rui Huo and Xia Li*

Department of Chemistry, Capital Normal University, Beijing 100048.

Lanthanide complexes with 6^3 topology net were synthesized. White light emissions were realized by Sm(III) complex and Ln(III) doped Eu(III) complexes.